ACI MATERIALS JOURNAL TECHNICAL PAPER

Title no. 90-M50

Fatigue Fracture of High-Strength Concrete and Size Effect

by Zdeněk P. Bažant and William F. Schell

Results of an experimental study of fatigue fracture of geometrically similar high-strength concrete specimens of very different sizes are reported and analyzed. Three-point bend notched beams 1.5, 4.24, and 12 in. deep were subjected to cyclic loading with a lower load limit of $0.07P_u$ and an upper limit between 0.73 and $0.84P_u$, where P_u = maximum load in monotonic loading. The number of cycles to failure ranged from 200 to 41,000. It is found that the Paris law for the crack length increment per cycle as a function of the stress intensity factor, which was previously verified for normal concrete, is also applicable to high-strength concrete. However, for specimens of different sizes, an adjustment for the size effect needs to be introduced, of a similar type as previously introduced for normal concrete. This size adjustment represents a gradual transition from crack growth governed by stress amplitude to crack growth governed by stress intensity factor amplitude. The structure size for which this transition occurs is found to be about an order of magnitude smaller for high-strength concrete than for normal concrete, which means that the fracture process zone under cyclic loading is much smaller and the behavior is much closer to linear elastic fracture mechanics (LEFM). A linear regression plot estimating the size-adjusted parameters is derived. An LEFM-type calculation of the deflections under cyclic loading on the basis of the size-adjusted Paris law yields correct values for the terminal phase but grossly underpredicts the initial deflections. Overall, the results underscore the importance of considering fatigue fracture growth in the case of high-strength concrete structures subjected to large, repeated loads, and taking into account the very high brittleness under fatigue loading.

Keywords: deflection; **fatigue (materials); fracture properties; high-strength concretes.**

Due to its more homogeneous microstructure, high-strength concrete is more brittle than normal strength concrete. This is most apparent from size effect tests, which showed that the response of typical fracture specimens made of high-strength concrete is very close to linear elastic fracture mechanics.[1]

The fracture properties of high-strength concrete have been studied for monotonic loading;[2,1,3] however, no information appears to exist for fatigue loading. Such loading is very important for bridges, offshore structures, and structures subjected to heavy wind loads or machinery. Cyclic loading causes cracks to grow, which results in a growth of deflections and, after a certain number of cycles, may cause failure. Fatigue fracture has previously been experimentally studied for normal strength concrete.[4-6] It has been found that the well-known Paris law giving the crack length increment per cycle as a function of the amplitude of the stress intensity factor is invalid for concrete, although it has been widely used for metals. However, after an adjustment for the size effect,[5] fatigue fracture of normal concrete can be described very well. The purpose of this work is to determine the laws that describe the fatigue fracture of high-strength concrete. Such laws are needed for predicting the growth of cracks in concrete structures under large repeated loads due to traffic, wind, thermal cycles, etc.

EXPERIMENTAL INVESTIGATION

The test specimens were made of a high-strength concrete that is typical for the Chicago area. The concrete mix was designed for compressive strength exceeding 12,000 psi. The ratios of the mix components to cement, by weight, were as follows: portland cement: 1.00, water: 0.316, fly ash: 0.132, silica fume: 0.0507, $\frac{3}{8}$-in. maximum-diameter crushed aggregate: 2.18, siliceous sand: 1.51, retarder: 0.00190, and superplasticizer: 0.00951.

Three fracture specimens of varying size were cast from the same batch of concrete. The specimens were three-point bend fracture specimens shown in Fig. 1. Specimens of different sizes were geometrically similar in two dimensions, having the same thickness b equal to 38.1 mm (1.5 in.) (as explained in previous works, it is preferable to keep the thickness constant, because this minimizes the differences in hydration heat and drying effects, as well as in the so-called wall effect and effect of curvature of the fracture front throughout the thickness). The beam depths were D = 38.1, 107.8, and 304.8 mm (1.50, 4.24, and 12.00 in.), and the ratio of the sizes was $1:\sqrt{8}:8$. The span L was $2.5D$, where D is the beam depth. The notch, cut by a band saw, had the length $a_0 = D/6$. Also, six companion cylinders with diameter 101.6 mm (4 in.) and length 203.2 mm (8 in.) were cast from the same batch. All the specimens were compacted, removed from the mold after 48 hr, and stored in a moist-curing room at 26 C for 56 days.

ACI Materials Journal, V. 90, No. 5, September-October 1993.

Received Apr. 27, 1992, and reviewed under Institute publication policies. Pertinent discussion will be published in the July-August 1994 *ACI Materials Journal* if received by Apr. 1, 1994.

Zdeněk P. Bažant, FACI, holds the W.P. Murphy professorial chair at Northwestern University, where he also served as Center Director and Structural Engineering Group Coordinator. He is a registered structural engineer in Illinois, consultant to Argonne National Laboratory, Editor of the ASCE Journal of Engineering Mechanics, *Regional Editor of the* International Journal of Fracture, *President of the Society of Engineering Science, founding President of the International Association of Fracture Mechnics for Concrete Structures (IA-FraMCos), and chirman of RILEM creep committee and of SMiRT Division H. He chaired ACI Committee 446, Fracture Mechanics. His latest honors: 1990 Gold Medal from the Building Research Institute of Spain, 1990 Humboldt Award, 1991 Honorary Doctorate from T.U. Prague, 1991 Best Engineering Book of the Year Award (for* Stability of Structures, *with L. Cedolin), 1992 Meritorious Publication Award from SEAOI, and 1993 Medal for Advances in Mechanics (Prague).*

***William F. Schell** is currently a structural engineer with Hopper and Associates, Redondo Beach, Calif. He received his BS in civil engineering from the University of California, Berkeley, and MS in structural engineering from Northwestern Univerisity. His research interests include fatigue and fracture applications to structural design.*

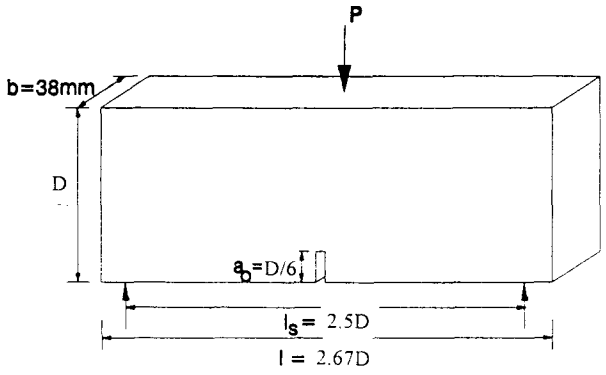

Fig. 1—Specimen geometry

The fatigue tests were conducted in a closed-loop, digitally controlled machine (MTS) with a 89,600 N (10 t) load capacity. The crack-mouth opening displacement (CMOD) was measured by an MTS extensometer. Data acquisition for both load and CMOD was performed by the computer controlling the test. The control variable was the load *P*.

The overall experimental setup for the largest specimen is shown in Fig. 2. To fit the largest beam in the testing frame, a stiff steel beam is used as the base. A photo of the frame with the medium specimen and configuration of the instruments is shown in Fig. 3.

The median age of the specimens at the time of test was 70 days, chosen higher than the usual 28 days to minimize the strength gain due to aging during the testing. All the tests were done within a span of 2 weeks. Companion cylinders tested just before and after the fatigue testing revealed a strength gain of only 3 percent, which was neglected in evaluating the tests.

Fatigue testing was preceded by compliance calibration of the fracture specimens. The compliance calibration method, verified for concrete in Reference 7, was used to determine the crack length during the loading cycles, because determination of the effective crack length by optical measurements is virtually impossible due to diffused cracking at the fracture front, as well as the curvilinear shape of the crack front through the specimen thickness, revealed by dye penetration tests. The compliance calibration method was shown to work

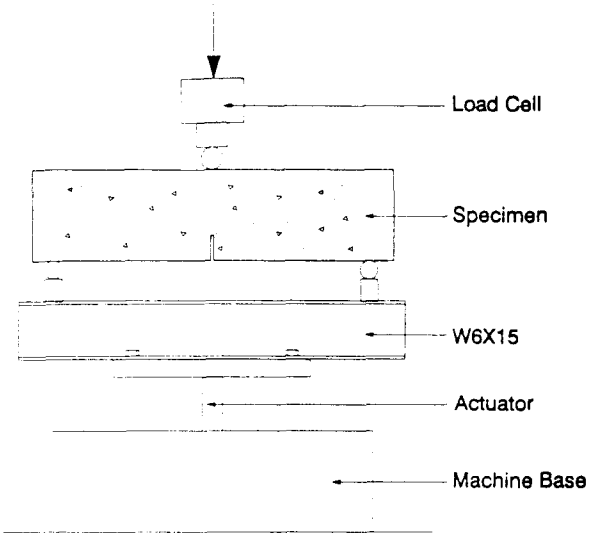

Fig. 2—Test setup for large specimen

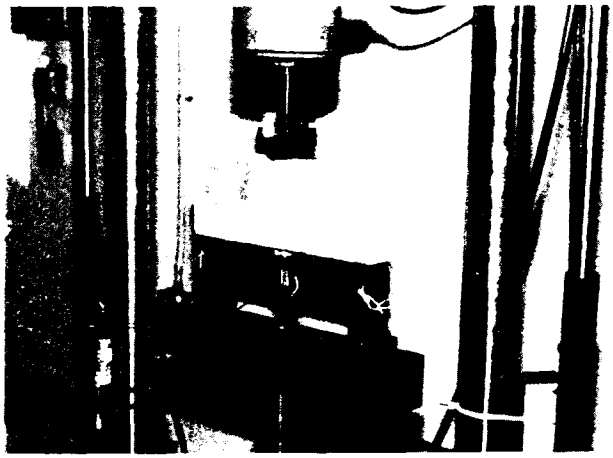

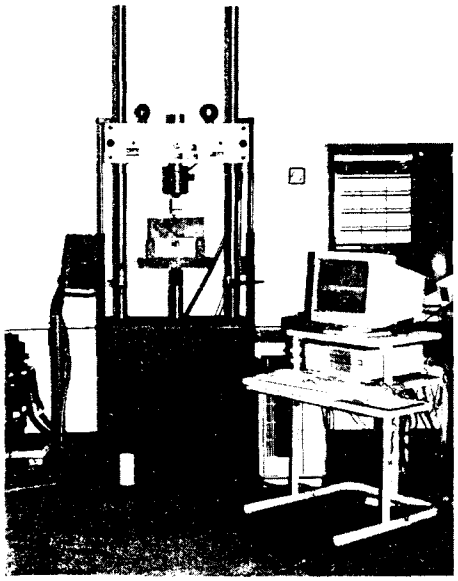

Fig. 3—Overall test arrangement and instrumentation of medium specimen

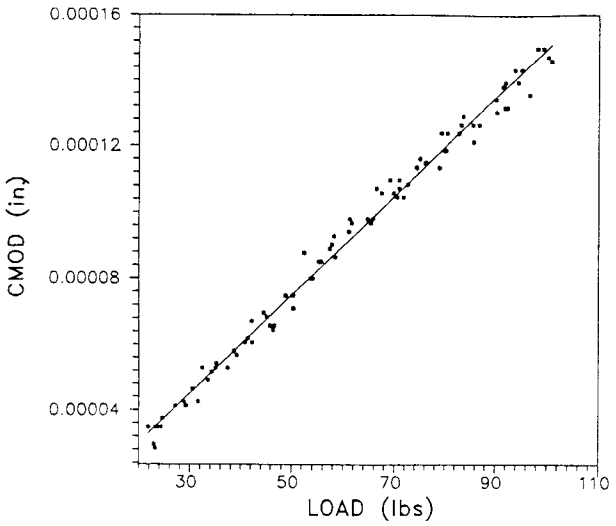

Fig. 4—Load-CMOD curve for compliance calibration method

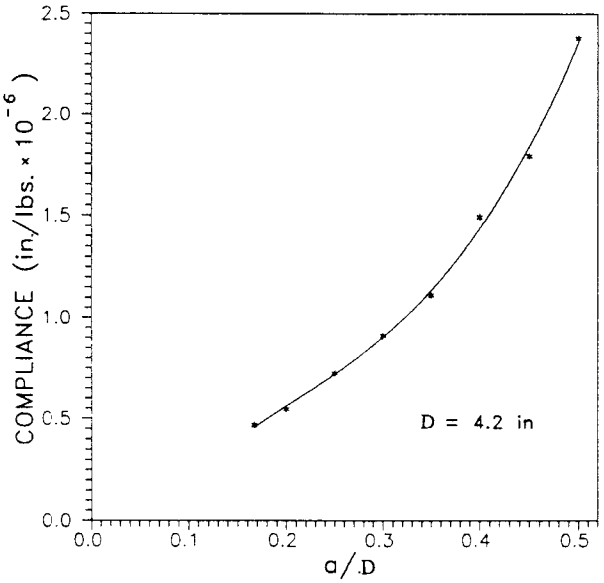

Fig. 5—Compliance calibration curve

for $a/D < 0.5$, which is sufficient for the present tests. The compliance calibration was done on the actual fatigue specimens, one calibration test for each size. The initial notch length, $a_o = D/6$, was the same as for the actual fracture specimens. Subsequently, making cuts with a band saw, the notch length was incremented. Each increment was assumed to remove the previously formed fracture process zone, which was rather small due to the small loads applied (the load was less than 20 percent of the maximum load). From such measurements, a plot of the load values versus crack-mouth opening displacement (CMOD) was obtained (Fig. 4) and a regression line was passed. The slope of the regression line is the compliance for the given crack length (actually it is not a compliance coefficient in the sense of an off-diagonal term of the compliance matrix, since the load P is not associated by work with CMOD). Repeating the tests shown in Fig. 4 for a range of crack lengths, the compliance calibration curve (shown in Fig. 5 for depth $D = 107.8$ mm = 4.24 in.) was obtained, one for each specimen size D. The elastic modulus values in the theoretical expression for the compliance curve are adjusted to obtain the best fit, as shown by the solid curve in Fig. 5. This curve is then used to estimate the corresponding crack length from the measured compliance during the fatigue test.

Table 1 — Peak loads and fatigue results

Size	P_u, N	P_{max}, percent*	N†	n	log C
Small	2940	73	33,409	8.64	−69.63
	2887	82	530	6.05	−49.44
		84	212	8.44	−65.22
Medium	5707	77	7450	9.99	−76.40
	6120	84	854	8.57	−67.30
Large	11,738	77	40,867	10.01	−79.77
	11,271	84	1348	9.61	−75.74

*P_{max} in percentage of ultimate load.
†N = number of cycles to failure.

Prior to fatigue tests, monotonic load-controlled tests were carried out to determine the maximum loads of the specimens. These tests were used to determine the material fracture parameters according to the size effect method[8] and decide the load values to be used in the fatigue experiments. The measured peak loads P_u in monotonic tests are given in Table 1. A typical load-CMOD curve for $D = 76.2$ mm (3 in.) is shown in Fig. 6 for the high-strength concrete used in the current experiments.

The Young's modulus of high-strength concrete was estimated from the approximate empirical formulas: $E = 3320 f_c' + 6900 = 38{,}300$ MPa (5550 ksi) and the tensile strength $f_u = f_r = 0.94 \sqrt{f_c'} = 8.9$ MPa (1290 psi), in which f_c' must be given in MPa. The compressive strength f_c' was determined by testing the companion cylinders according to ASTM standards; its average value at the beginning of the fatigue tests was 90.3 MPa (13,100 psi). The fracture parameters, obtained by the size effect method from the ultimate loads of specimens of various sizes measured under monotonic loading, were: fracture toughness $K_{IF} = 44.7$ N mm$^{-3/2}$; fracture energy $G_f = 52.1$ N/m; transitional size in the size effect law $D_0 = 31.8$ mm; and effective length of the fracture process zone in an infinitely large specimen $c_f = 7.6$ mm $= 0.8\, d_a$, where d_a is the maximum aggregate size = $^3/_8$ in. (note that the value of c_f is relatively small, which is the reason for the high degree of brittleness of high-strength concrete).

The fatigue tests were conducted at two different values of the upper load limit P_{max}, equal to $0.75P_u$ and $0.85P_u$. The minimum load limit was approximately $0.07P_u$ in all the tests (it was necessary to maintain a nonzero load to avoid separation between the specimen and the loading fixture). Maximum and minimum load limits were constant during the fatigue tests. The frequency chosen was 10 Hz. This is much higher than the frequency of 0.04 Hz used by Bažant and Xu,[5] but it appears that the frequency has a secondary influence compared to the influence of the number of cycles (although this might not be true for cycle periods stretching over months and years). Despite the high frequency, no measurement or stability problems were encountered during the test. The com-

puter data acquisition system recorded the load, CMOD, stroke, and cycle number for every peak and valley of the load history.

ANALYSIS OF RESULTS

The results of the fatigue tests are given in Table 1. The tests also include different load levels ranging from 73 to 84 percent of P_u (ultimate load in monotonic loading). It is seen from Table 1 that even such relatively small differences in the upper load limit lead to enormous differences in number of cycles to failure (ranging from 200 to 41,000). The loading system was not capable, at the fast rate of loading, to produce exactly the desired load limit in the cycle P_{max} set at the controls. This is why the recorded P_{max} values are slightly different. The evaluation was, of course, based on the actual measured P_{max}.

A typical plot of the relative crack length $\alpha = a/D$ versus the number of cycles N for the middle-size specimen is presented in Fig. 7(a). Considerable random differences among the results were encountered for the largest specimens; Fig. 7(b) shows that in one specimen the crack virtually did not grow until close to failure, while in another specimen the crack grew almost uniformly throughout the duration of the test (but the failure occurred after approximately the same number of cycles). Probably these differences are due to errors of control and measurement. Nevertheless, the mean trend described by these scattered results matches the other tests and agrees with the present theory. However, since only five specimens were tested for the two different upper load limits, more extensive testing is desirable in the future.

For many materials, the crack length increment per cycle approximately follows the empirical Paris law,[9,10] which is normally written as $\Delta\alpha/\Delta N = C_0\ (\Delta K_I)^n$ (C_0 replaces Paris' notation C to avoid any confusion with compliance). This law can be rewritten in the nondimensional form as[5]

$$\frac{\Delta a}{\Delta N} = \kappa\left(\frac{\Delta K_I}{K_{Ic}}\right)^n \qquad (1)$$

in which $\kappa = C_0 K_{Ic}^n$; ΔK_I is the amplitude of the stress intensity factor for the current crack length a; κ or C_o and n = empirical constants; and K_{Ic} fracture toughness for monotonic loading = a critical value of K_I for monotonic loading, which is introduced for the convenience of dimensionality. The stress intensity factor is calculated from the applied load P, using the well-known formula of linear elastic fracture mechanics

$$K_I = \frac{Pf(\alpha)}{b\sqrt{D}} \qquad (2)$$

in which $\alpha = a/D$ = relative crack length; for the present three-point bend specimen, $f(\alpha) = 6.647\alpha^{1/2}(1 - 2.5\alpha + 4.49\alpha^2 - 3.98\alpha^3 + 1.33\alpha^4)/(1-\alpha)^{3/2}$ (which was obtained by curve-fitting of finite element results).[1] For other specimen geometries, function $f(\alpha)$ can be found in fracture textbooks and handbooks.[11,12] Using $f(\alpha)$, one has 5 $C_f = D_0 g(\alpha_0)/g'(\alpha_0)$ where $g(\alpha) = f^2(\alpha)$.

The validity of the Paris law [Eq. (1)] has been extensively verified for metals, and recently it has also been shown applicable to normal concrete.[5] However, it has been found that, in contrast to the previous experience with metals, the value of K_{Ic} cannot be kept the same for very different specimen sizes. It appeared that a good agreement with the test results for different sizes can be obtained if the value of K_{Ic} is considered to be a function of the specimen size and the law governing K_{Ic} is taken to be the same as that ensuing from the size effect law for ultimate loads in monotonic tests, as proposed in References 13 through 15. This previously derived law has the following form

$$K_{Ic} = K_{If}\sqrt{\frac{\beta}{1+\beta}} \qquad (3)$$

in which $\beta = D/D_o$ = relative specimen size (also called the brittleness number since it determines the proximity to linear elastic fracture mechanics) and K_{If} = a constant which represents the asymptotic value of fracture toughness for an infinitely large specimen coinciding with the asymptotic value of the R-curve. D_o is an empirical constant that may be interpreted as the size in the middle of the transition between the

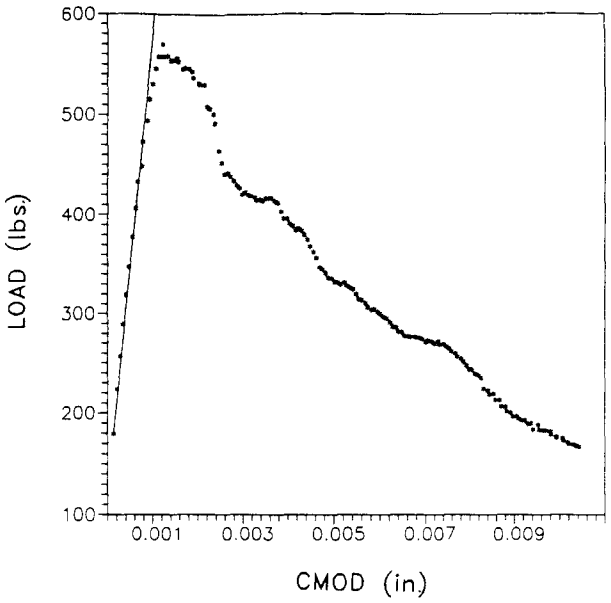

Fig. 6—Typical load-CMOD curve for high-strength concrete specimens used, D = *76.2 mm*

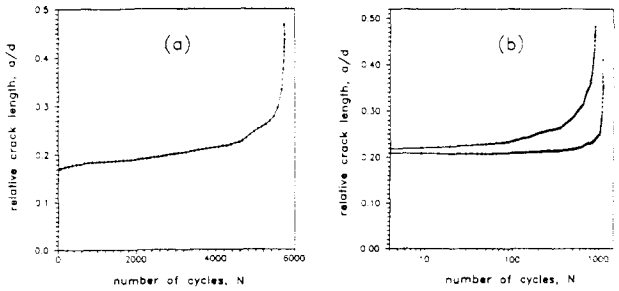

Fig. 7—Typical plots of relative crack length versus number of cycles N *recorded for (a) one medium and (b) two large specimens*

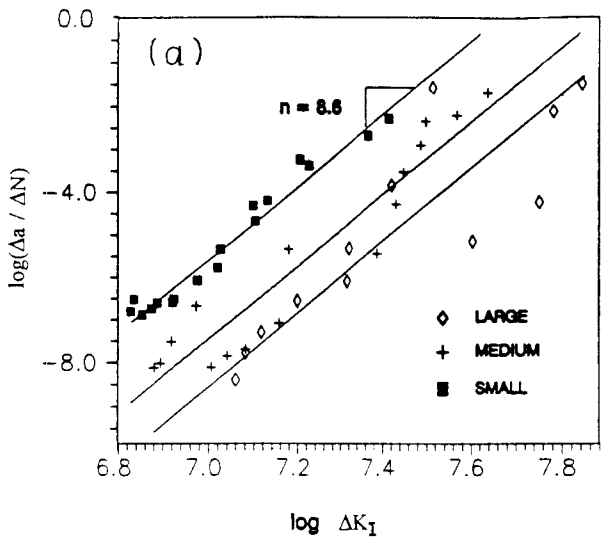

Fig. 8(a)—Linear regression according to original Paris Law (data points refer to individual specimens)

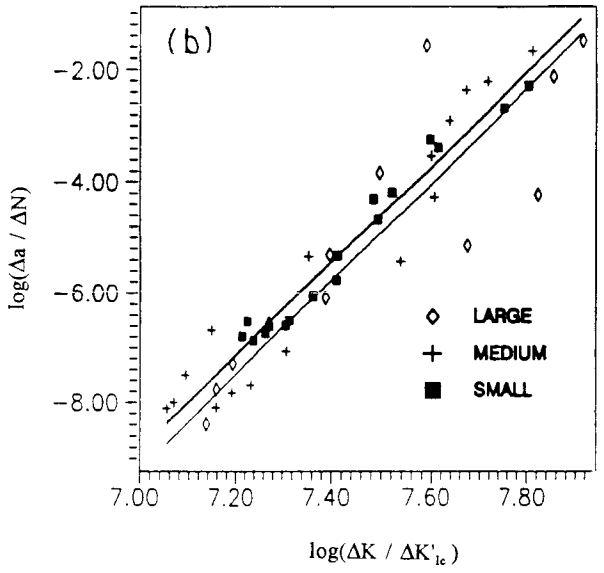

Fig. 8(b)—Linear regression according to size-adjusted Paris law (data include two specimens per size)

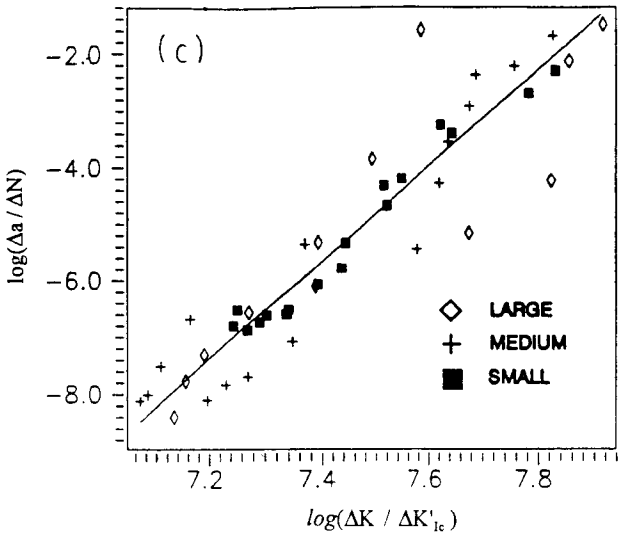

Fig. 8(c)—Linear regression with optimal fit (data include two specimens per size)

strength theory and linear elastic fracture mechanics. For $D \ll D_o$ ($\beta \ll 1$), Eq. (1) is equivalent to crack growth being proportional to the nth power of the nominal stress amplitude [Eq. (10), Reference 5], while for $D \gg D_o$ ($\beta \gg 1$), the crack growth per cycle according to Eq. (1) depends only on the amplitude of the stress intensity factor, as in the classical Paris law (which is asymptotically approached for sufficiently large sizes).

The size-adjusted Paris law [Eq. (3)] has been verified for normal concrete but not, however, for high-strength concrete. Eq. (1) can be reduced to a linear regression plot by plotting log ($\Delta a/\Delta N$) versus log(ΔK), as a means of size adjustment, versus log($\Delta K/K_{Ic}$). The slope of the regression lines in all the figures is the same (taken as the average value of the regression slopes for individual sizes); the slope is $n = 8.6$, which is a slightly smaller value than that obtained from normal concrete, which was $n = 10.6$. Fig. 8(a) shows the plot of the present test results for all specimen sizes when the value of K_{Ic} is replaced by $K'_{If} = 1.0$, as in the original (unadjusted) Paris law [Eq. (1)]; the regression lines represent the optimal fits obtained separately for each specimen size. The fact that these regression lines do not coincide and are not even close indicates that the original Paris law is not valid.

When the size adjustment according to Eq. (1) is introduced and the value of D_o equal to the monotonic value (31.8 mm) obtained from the size effect method is used, one obtains the plot shown in Fig. 8(b) in which $K'_{Ic} = K'_{If}[\beta/(1+\beta)]^{1/2}$ = relative values of K_{Ic} from Eq. (3) (note that two of the three straight lines nearly coincide). The fact that the regression lines for different sizes are now very close to each other confirms that the size-adjusted Paris law [Eq. (1)] is valid. Furthermore, Fig. 8(c) shows the plot when all the results are fitted by the same regression line, for which $D_o = 1.5d_o$ where d_o is the value for monotonic loading.[15] For normal strength concrete, the value of $D_o = 10d_o$ was found.[5] Since D_o is proportional to the length of the fracture process zone from the size effect method, it can be concluded that the fracture process zone is much smaller in high-strength concrete than in normal concrete during fatigue loading.

Note that Eq. (1) and (3) yield

$$\Delta K_I = K_{If}\left(\frac{1}{\kappa}\frac{\Delta a}{\Delta N}\right)^{\frac{1}{n}}\sqrt{\frac{\beta}{1+\beta}} \qquad (4)$$

This equation can further be algebraically rearranged to the linear regression plot

$$Y = A_1 + B_1 X \qquad (5)$$

in which

$$Y = \left(\frac{\Delta a}{\Delta N}\right)^{\frac{2}{n}}\Delta K_I^{-2}, X = \frac{1}{D} \qquad (6)$$

$$A_1 = \kappa^{\frac{2}{n}} K_{If}^{-2}, B_1 = \kappa^{\frac{2}{n}} K_{If}^{-2} D_0 \tag{7}$$

Passing a regression line of measured Y-points versus X, one obtains the values of slope B_1 and Y-intercept A_1 from which one can evaluate

$$\kappa = A_1^{\frac{n}{2}} K_{If}^{n}, D_0 = \frac{B_1}{A_1} \tag{8}$$

The result is $D_o = 1.42d_o$, which is close to the value $1.5d_o$ found from nonlinear optimization. This linear regression is an alternative to the direct nonlinear optimization in the plot of the Paris law in Fig. 8(c), which is nonlinear. However, with a nonlinear optimization subroutine such as the Marquardt-Levenberg algorithm, direct determination of D_o and κ is also quite easy.

DEFLECTION CURVE

Comparison of the calculated and measured deflection curve is the easiest and most unambiguous check of the fracture formulation for monotonic loading. For the special case of rate-independent elastic behavior and monotonic loading, the curve of load P versus load-point deflection u of a fractured specimen is given by the following well-known relations[16]

$$u = \frac{P}{E}\bar{C}(a), \alpha = \frac{a}{D} \tag{9}$$

$$\bar{C}(a) = \bar{C}_o + \frac{2}{b}\varphi(\alpha) \tag{10}$$

$$\varphi(\alpha) = \int_0^{\alpha} [f(\alpha')]^2 d\alpha' \tag{11}$$

$$P = b\sqrt{D}\,\frac{K_{Ic}}{f(\alpha)} \tag{12}$$

in which $\bar{C}(a)$ is the unit load-point compliance (i.e., compliance for unit value of elastic modulus E) and $\bar{C}_o$ is the initial unit compliance at $a = a_o$. To determine the monotonic load-deflection curve, one chooses a series of values of the crack length a, and calculates u from Eq. (10) and (11) and P from Eq. (12). Thus, Eq. (10) through (12) define the load-deflection curve parametrically.

For fatigue loading, the load-deflection curve may be calculated similarly to Eq. (10) through (12). From Eq. (1), we express ΔN as a function of $\Delta\alpha$ and substitute the expression $\Delta K_I = \Delta P f(\alpha)/\sqrt{D}$. Integration then yields

$$N(\alpha) = \frac{1}{\kappa}\left(\frac{K_{Ic} b\sqrt{d}}{\Delta P}\right)^n \int_0^{\alpha} [f(\alpha')]^{-n} d\alpha' \tag{13}$$

Eq. (10) can be rewritten in the form

$$\Delta u = \frac{PD}{E}\left[\frac{d\bar{C}(a)}{da}\right]\Delta\alpha \tag{14}$$

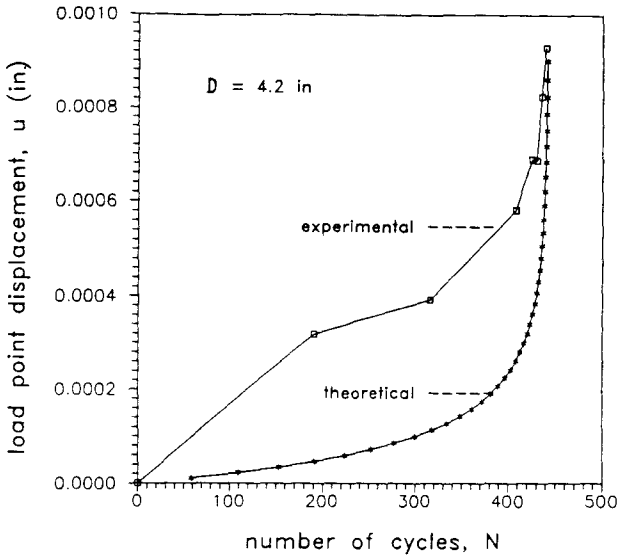

Fig. 9—Measured and calculated load-point displacements for medium-size specimen

Thus Eq. (13) and (14) define the load-deflection curve for cyclic loading. Choosing a sequence of values of α, one can calculate from Eq. (13) the number of cycles to reach this value and the corresponding displacement value from Eq. (14).

The load-point deflection curve calculated in this manner is shown in Fig. 9. For comparison, the experimental curve is also plotted. At the end there is a good agreement, but at the beginning of the test there is a large discrepancy. To eliminate this discrepancy is probably beyond the capability of the present theory, which represents a generalization of LEFM to fatigue. Probably it will be necessary to make generalizations akin to the R-curve for monotonic loading that take into account in a simplified manner the growth of the apparent fracture toughness associated with the growth of the process zone size.[17]

CONCLUSIONS

1. As previously shown for normal concrete, the Paris law is also applicable to high-strength concrete, but only if the specimen sizes do not vary significantly.

2. For a broad range of specimen or structure sizes, the Paris law needs to be adjusted in the same manner as previously proposed for normal concrete. The classical, unadjusted Paris law is approached asymptotically for large specimen sizes.

3. The transitional size D_o of the size adjustment of the Paris law has a value rather close to that for monotonic fracture, while previous investigations of normal concrete indicated this value to be an order of magnitude higher. This means that the behavior of typical laboratory fracture specimens of high-strength concrete under cyclic loading is quite close to linear elastic fracture mechanics, while that of normal concrete was previously found roughly in the middle of the transition between the strength theory and linear elastic fracture mechanics. This further implies that the fracture process zone under cyclic loading is in high-strength concrete about